Hindawi
Scientific Programming
Volume 2021, Article ID 9988823, 13 pages
https://doi.org/10.1155/2021/9988823

Research Article

A Novel Adaptive Mutation PSO Optimized SVM Algorithm for sEMG-Based Gesture Recognition

Le Cao,[1] Wenyan Zhang,[1] Xiu Kan,[1,2] and Wei Yao[1]

[1]*School of Electronic and Electrical Engineering, Shanghai University of Engineering Science, Shanghai 201620, China*
[2]*School of Mathematics, Southeast University, Nanjing 210096, China*

Correspondence should be addressed to Xiu Kan; xiu.kan@sues.edu.cn

Received 16 March 2021; Revised 3 June 2021; Accepted 9 July 2021; Published 17 July 2021

Academic Editor: Shah Nazir

In the field of noncontact human-computer interaction, it is of crucial importance to distinguish different surface electromyography (sEMG) gestures accurately for intelligent prosthetic control. Gesture recognition based on low sampling frequency sEMG signal can extend the application of wearable low-cost EMG sensor (for example, MYO bracelet) in motion control. In this paper, a combination of sEMG gesture recognition consisting of feature extraction, genetic algorithm (GA), and support vector machine (SVM) model is proposed. Particularly, a novel adaptive mutation particle swarm optimization (AMPSO) algorithm is proposed to optimize the parameters of SVM; moreover, a new calculation method of mutation probability is also defined. The AMPSO-SVM model based on combination processing is successfully applied to MYO bracelet dataset, and four gesture classifications are carried out. Furthermore, AMPSO-SVM is compared with PSO-SVM, GS-SVM, and BP. The sEMG gesture recognition rate of AMPSO-SVM is 0.975, PSO-SVM is 0.9463, GS-SVM is 0.9093, and BP is 0.9019. The experimental results show that AMPSO-SVM is effective for low-frequency sEMG signals of different gestures.

1. Introduction

Surface electromyography signal is the superposition of action potentials of multiple active motor units in time and space during muscle contraction. Skeletal muscle activity can be measured and predicted by sEMG signal. Different gesture actions have different action potentials. Different gesture actions can be distinguished by analyzing the differences between action potentials [1]. Hand gesture recognition based on sEMG has been widely used in the diagnosis of skeletal muscle system diseases, rehabilitation medicine, biological feedback, and human-computer interaction, especially in the field of sEMG prosthetic control [2–4]. There are many methods and researches on gesture recognition based on sEMG now, which mainly focus on signal feature extraction, feature selection, and classification [5].

Feature extraction is a key step in EMG control. EMG control requires accurate recognition, so every link is designed to minimize the error. The capability of a recognition system is directly related to feature selection [6]. For the EMG control system, how to extract effective feature information and make full use of the characteristics of the signal to characterize the EMG signal is the main problem to be solved. According to the theory of pattern recognition [7–9], the feature extraction methods of EMG signal are mainly as follows: time domain analysis method, frequency domain analysis method, time-frequency analysis method, time series analysis method, and nonlinear dynamics analysis method [10–13]. In motion control, in addition to the accuracy of recognition, the time used for recognition is also essential. The time domain analysis method deals with the EMG signal as a function of time and obtains the statistical characteristics of the signal. Time series refers to a group of data arranged in time order. Time series analysis is a data processing method that uses a parameter model to analyze and process the observed ordered random data. In recent years, the parametric model method has become an important solution for surface electromyography signal analysis because of its high-frequency resolution, among

which AR model method is a typical one. AR model is a linear, second-order moment stationary model, which is suitable for short data analysis and convenient operation, especially for real-time processing of EMG control. The extraction of time domain features and model coefficients is relatively simple and the calculation is relatively fast.

In order to retain more information of EMG signal, the number of channels of EMG signal acquisition instruments reaches 8 or more, which leads to the problem of the high dimension of the signal after feature extraction. In order to reduce the disaster of high dimension feature operation and preserve the global characteristics of the signal, it is necessary to use the dimension reduction algorithm for feature selection. During the past few years, feature selection methods have been under intensive research by using various types of methods, such as principal component analysis (PCA) [14], unsupervised clustering [15], and rough set theory [16]. After the feature information of the signal is obtained, the selection of the classifier is followed to determine the accuracy of signal recognition.

Gesture recognition is one of the algorithms of EMG pattern recognition. EMG pattern recognition is normally divided into three stages [17]. The third stage is classification, which establishes a model for gesture classification. Gesture classification is the switch of motion control. The first step of motion control is to recognize the motion intention in the form of gesture correctly. Gesture recognition is the key step to complete the follow-up work, including force prediction and motion control. On the other hand, one of the key problems in gesture pattern recognition is to identify the motion type of the sEMG signals. Machine learning and deep learning are widely used for data processing. There are many pattern classification methods used in sEMG, including K-nearest neighbor (KNN), artificial neural network (ANN), and support vector machine [18–23].

However, the research on the above features extraction and gesture recognition focuses on the surface muscle electrical signals with high sampling frequency. With the development of Bluetooth communication and low-power embedded technology, wearable sensors begin to play a role in gesture recognition. Gesture recognition based on the wearable sensor is generally robust and accurate and is becoming an important part of the motion control platform [24]. It is very popular to use convenient and comfortable wearable devices for gesture recognition and motion control. For example, MYO bracelet is a noninvasive surface electromyography acquisition method developed by Thalmic laboratory. It provides a more convenient interface for motion control based on human gesture recognition. However, wearable sensors (such as MYO bracelet) have the lower sampling frequency than the widely used 1 kHz EMG acquisition devices. Gesture recognition methods based on high-frequency sEMG signals have been quite mature, but these methods are not suitable for sEMG signals below 1 kHz. Reference [25] uses SVM to classify sEMG signals obtained at 200 Hz and 1 kHz sampling frequency, and the classification accuracy of 1 kHz is obviously higher than 200 Hz. In reference [26], the prosthetic hand of the forearm amputee is controlled by a surface electromyography signal with a frequency of 1 kHz. The motion control based on low sampling rate is still less accurate, and how to maintain high classification accuracy is a key point.

Motivated by the above discussion, an AMPSO optimized SVM algorithm is proposed, which is successfully applied to the recognition of sEMG signals with a low sampling rate. The main contributions of this paper can be summarized from the following three points:

(1) A novel adaptive mutation method is proposed to improve the original PSO algorithm; moreover, a new calculation method of mutation probability is introduced in this paper

(2) A combined gesture recognition method based on a low sampling rate EMG signal is proposed, which has the advantages of simple calculation, fast acquisition speed, and high classification accuracy

(3) A feature selection strategy, which can effectively remove the redundancy between features and improve the accuracy of subsequent sEMG classification algorithms, is designed to solve the problem of high feature dimension

The rest of this paper is arranged as follows. In Section 2, it discusses the feature extraction method of sEMG gesture recognition task. In Section 3, it introduces the AMPSO-SVM algorithm for sEMG pattern classification and demonstrates the process of adaptive PSO mutation in detail. In Section 4, the comparative experiments are developed to demonstrate the effectiveness of the proposed AMPSO-SVM method. Finally, it summarizes the research work in Section 5.

2. Feature Extraction and Selection

As shown in Figure 1, we design a combination method for sEMG gesture classification. This combination is suitable for EMG signals with low sampling rate and high dimension. This proposed algorithm is efficient with few parameters. Moreover, the parameters of SVM are selected automatically by AMPSO to avoid complicated calculations.

Specific time domain and time series features are extracted from the sEMG signals after the denoise through the proposed combination. After feature extraction, the high-dimensional samples are selected by GA and finally sent to AMPSO-SVM classifier for gesture classification.

2.1. Feature Extraction. Feature extraction is an essential step in EMG gesture pattern recognition. The purpose of feature extraction is to distinguish different gesture actions as far as possible, which is directly related to the discrimination ability of the gesture recognition system. Features or attributes of EMG signals representing various upper limb movements are extracted. The feature processing includes three steps: noise reduction, maximum contribution feature determination, and normalization.

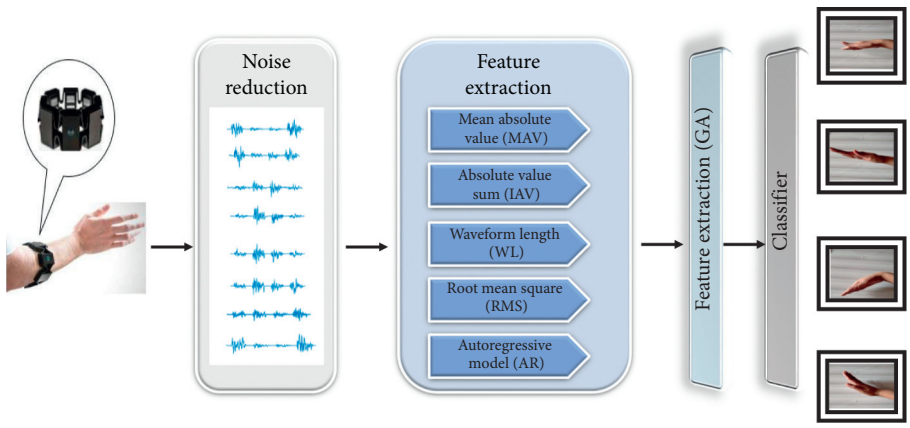

Figure 1: EMG signal processing flow.

2.1.1. Noise Reduction. The practical process of data acquisition will always evolve the noise due to the environmental impact. The existence of noise often conceals the information of the data. Therefore, it is necessary to preprocess the actual signals, and the most important step of preprocessing is noise reduction [27]. DB44 wavelet method is selected to decompose the data into five levels, and the five-layer wavelet coefficients are obtained as the data before feature extraction. Figure 2 shows the waveform of one channel EMG signal after denoising.

2.1.2. Maximum Contribution Feature Determination. The actions in this dataset are hand at rest, hand clenched in a fist, wrist flexion, wrist extension, radial deviations, ulnar deviations, and extended palm (the gesture was not performed by all subjects). The main local structures of the wrist are radial carpal tunnel, ulnar carpal tunnel, and carpal tunnel. The related muscles were flexor carpi ulnaris, flexor carpi radialis, extensor carpi longus radialis, extensor digitorum, and extensor carpi ulnaris. When the muscle contraction force slightly changes, the RMS, MAV, and other time domain characteristics of sEMG signal change greatly, and the AR coefficient can accurately estimate the power spectrum of the signal. The position of the electrode on the muscle surface almost does not affect the coefficient and can be less disturbed by the external environment. Based on the physiological information of muscle, the researchers select the characteristics with strong correlation with muscle contraction and relaxation state in clinical manifestations that include mean absolute value (MAV), integrated absolute value (IAV), waveform length (WL), root mean square (RMS), and autoregressive model (AR) [28–32]. The physiological explanations of the five characteristics which are closely related to muscle contraction are shown in Table 1.

The sliding window is 200 and the step size is 50 (in sampling points). The overlap rate is 75%. The definition formulas for the selected feature are as follows:

$$\begin{aligned}
\mathrm{RMS} &= \sqrt{\frac{1}{M}\sum_{k=1}^{M} x_k^2},\\
\mathrm{MAV} &= \frac{1}{M}\sum_{k=1}^{M} \left|x_k\right|,\\
\mathrm{IAV} &= \sum_{k=1}^{M} \left|x_k\right|,\\
\mathrm{WL} &= \frac{1}{M}\sum_{k=1}^{M-1} \left|x_{(k+1)} - x_k\right|,\\
x_k &= -\sum_{i=1}^{P} a_i x_{k-i} + \omega_k,
\end{aligned} \tag{1}$$

where $x_k (k = 1, 2, \ldots, M)$ is the time series of the signals, $P = 7$ is the order of AR model (the best result is the 7th order AR coefficient), a_i is the parameter of AR model, and ω_k is a white noise. In this paper, the Burg method is used to select the parameters of AR model $a_1 - a_7$.

In the process of the experiment, 88-dimensional feature sample data are extracted at once; five features are extracted from each channel of MYO bracelet. In other words, one dimension is extracted from each channel of MAV, IAV, WL, and RMS, and seven dimensions are extracted from each channel of AR model.

2.1.3. Data Normalization. Data normalization is a primary work of data processing. Different evaluation indexes often mean different dimensions and dimension units, which will affect the results of data analysis. To eliminate the dimensional influence between indexes, data normalization processing is needed to solve the comparability between data indexes. In this paper, the [0, 1] interval normalization is set for the EMG dataset. The comparison of classification accuracy with and without normalization is shown in Table 2,

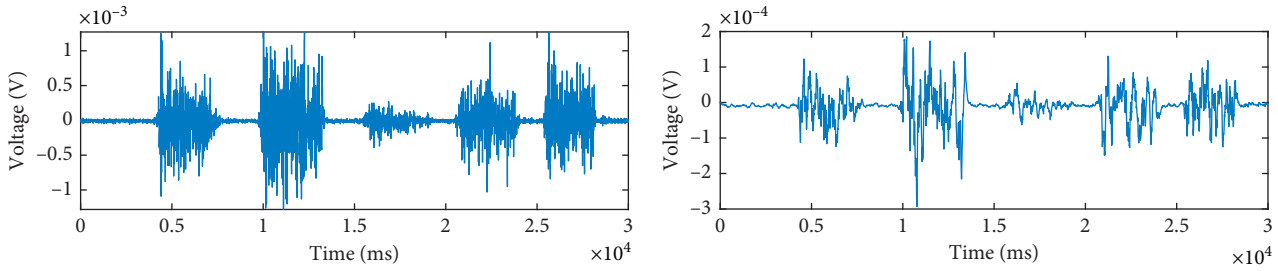

Figure 2: Surface electromyography signal after noise reduction. (a) Original signal. (b) Signal after denoising.

Table 1: Physiological explanation of characteristics.

Features	Physiological explanation
RMS	RMS mainly reflects the type of motor units and the degree of synchronization during muscle activity
MAV	MAV is well matched with the change of muscle tension and also reflects the change of muscle contraction
IAV	IAV is the characteristic after all the amplitude of the signal is converted into the positive value; it is the most intuitive response of muscle contraction force; the larger the IAV is, the greater the muscle contraction force is
WL	WL can reveal the change of amplitude, frequency, and duration of EMG waveform
AR	EMG spectrum changes with the change of muscle contraction state, which will cause the change of AR model coefficient; by monitoring the AR model coefficient, the muscle contraction state can be estimated

Table 2: Normalized comparison.

Selected normalization method	Classification accuracy of test set (%)
[0, 1] interval normalization	94.8148
No normalization	58.9815

where $C = 31$ and $\sigma = 0.01$ are set as in the reference. Table 2 illustrates that the classification accuracy is significantly improved from 58.9815% without the normalization to 98.8148% with [0, 1] interval normalization.

2.2. Feature Selection. If the dimension of the feature matrix is too large, it will put forward higher requirements for subsequent gesture recognition. Therefore, the computation of the feature matrix must be within the computational load of the computer. In this paper, we use a genetic algorithm as the feature selection method, and the recognition rate of k-nearest neighbor classification is used as the fitness function. A genetic algorithm needs to map the solution space to the coding space, and each binary code corresponds to a chromosome. The detailed steps of feature selection are shown as follows.

Initialization: in this paper, the coding length is designed to be 88, each bit in the chromosome represents a channel feature, and the gene of the chromosome is only available for the numbers of "0" or "1." If the corresponding position is "1," then the channel feature is selected; otherwise, the channel feature is discarded.

Calculate fitness function: the input feature matrix is divided into the training set and test set. For each feature combination, the training samples and test samples are reconstructed using the selected features. We use KNN to identify the test samples and obtain the recognition rate R. Let $f(X)$ be the fitness value, count be the number of predicted correct samples, and P be the number of test samples. The fitness value formula can be defined as follows:

$$f(X) = \frac{\text{count}}{P}. \tag{2}$$

Selection operation: the selection operation adopts the proportional selection operator. Set n as the number of individuals and M the sum of fitness. The fitness of all individuals in the population is summed as follows:

$$M = \sum_{k=1}^{n} f(X_k). \tag{3}$$

Meanwhile, the relative fitness value of each individual in the population can be calculated as follows:

$$m_k = \frac{f(X_k)}{M}, \quad k = 1, 2, \ldots, n, \tag{4}$$

where m_k represents the probability that the individual is selected and successfully inherited to the next generation. Roulette function is used to generate a random number between (0, 1) that is used to determine the number of times for each individual. Individuals with higher fitness values are more likely to be selected to pass on their genes to the next generation.

Cross operation: the single point crossover operator is used in the crossover operation process, randomly selects the same position of two individuals among the selected individuals, and exchanges positions according to a certain probability.

Mutation operation: mutation operation adopts the simplest single point mutation operator. Firstly, the mutation points are randomly generated, and then the gene value on the locus is changed according to the position of the mutation point. The binary coding is carried out in this scheme and the corresponding result of mutation operation can only change between "0" and "1."

Let the maximum evolutionary algebra be 40, the maximum population size M be 20, the chromosome length be 88, crossover probability pc = 0.3, and mutation probability pm = 0.03. The pseudocode of the genetic algorithm is shown in Algorithm 1.

The most representative combination of input variables can be selected after the proposed interactive evolution. Using the genetic algorithm to select 88-dimensional feature components, whose feature is retained, finally, only 44-dimensional feature components are retained. After the feature samples are determined, the method of machine learning is used to recognize the gesture.

3. Recognition Model

A 44-dimensional feature vector is obtained after the feature selection process, which is sent to the feature classifier for feature recognition and classification. The dataset used in this study uses MYO bracelet to measure. MYO bracelet has eight channels, and its dimension is relatively high. The sampling frequency of MYO bracelet is 200 Hz, and the number of data samples is small. Therefore, MYO EMG data contains characteristics of few samples and high dimensions. SVM is an effective classifier in solving small sample, nonlinear, and high-dimensional pattern recognition problems [33, 34]. Therefore, SVM and the obtained feature sample have a good combination. In this section, adaptive particle mutation with the design scheme of AMPSO-SVM model is used for sEMG gesture recognition. The flowchart of AMPSO-SVM gesture recognition algorithm is shown in Figure 3.

3.1. SVM. The existing methods for action pattern recognition of sEMG signals are basically based on the nonlinearity and nonstationarity of sEMG signals; however, these characteristics are not combined with the sample size, feature dimension, and the points that may fall into local minima to construct classifiers. SVM is capable of solving nonlinear, small sample, high dimension, and local minimum problems. In this paper, SVM theory is applied to the action pattern recognition of sEMG signal; moreover, a more effective action pattern recognition method of sEMG signal is discussed. SVM algorithm was originally designed for binary classification problems. When dealing with multiclass problems, it is necessary to construct appropriate multiclass classifiers. The method is proposed to design an SVM between any two samples; therefore, the samples of k categories require $k(k-1)/2$ times SVM. When an unknown sample is classified, the category with the most votes is the class of the unknown sample. The original spatial sample data are mapped to the high dimension through a nonlinear transformation with the kernel function for the linear nonseparable problem of SVM. In this paper, the researchers select the following radial basis function (RBF) [35–37] as the SVM kernel function:

$$K(x_i, x) = \exp\left(-\frac{1}{\sigma}\|x_i - x\|^2\right),$$
$$\lambda = \sum_{i=1}^{n} \alpha_i y_i K\left(x_i, x_j\right). \tag{5}$$

Therefore, SVM can be transformed into the following optimization problems:

$$\min \frac{1}{2}\sum_{i=1}^{j}\sum_{j=1}^{l} y_j \alpha_j - \sum_{j=1}^{l} \alpha_j, \quad 0 \le \alpha_i \le C, \tag{6}$$

where σ is the kernel function parameter, which implicitly determines the distribution of data after mapping to the new feature space; C is the penalty parameter, which is used to adjust the weight of the margin size and classification accuracy preference in the optimization direction. Penalty parameters C and kernel function parameters σ affect the classification accuracy and the stability of the SVM classifier. Since traditional parameter optimization methods, such as grid search method and gradient descent method, are easy to fall into local optimum in the process of optimization, and manual parameter adjustment causes a large error. Therefore, it is necessary to introduce a suitable parameter search method to find the sum of parameters in SVM. The problem has also been studied by previous researchers [38, 39]. The particle swarm optimization (PSO) algorithm is used in this paper to find the optimal parameters that are capable of improving the accuracy of the model classification and anti-interference ability.

3.2. AMPSO-SVM. In the past several years, biological evolutionary algorithms have been used to optimize the parameters of classifiers including the drosophila algorithm, genetic algorithm, gravity search algorithm, and particle swarm optimization algorithm [40–43]. Particularly, PSO as a global search evolutionary algorithm is proposed by Kennedy and Eberhart in 1995 [44]. Considering that SVM classifier is sensitive to penalty parameter and kernel radius parameter and it is difficult to find the appropriate parameters artificially, particle swarm optimization algorithm is introduced to optimize SVM classifier to find the appropriate parameters. In each iteration, particles update their positions and velocities according to the following equations:

$$v_{id}^{(k+1)} = \omega v_{id}^{k} + c_1 \text{rand}\left(p\text{best}_{id}^{k} - x_{id}^{k}\right) + c_2 \text{rand}\left(g\text{best}_{id}^{k} - x_{id}^{k}\right), \tag{7}$$

$$x_{id}^{(k+1)} = x_{id}^{k} + v_{id}^{(k+1)}, \tag{8}$$

where c_1 and c_2 are acceleration coefficients, adjusting the maximum step size to the global best particle and the

Initialization;
$k = 0$;
  while k to maximum iterations do
    while k = 1 to M do
      Calculate the fitness of population $f(X)$ according to formula (6);
    end while
  while k = 1 to M do
    Select operation to population;
  end while
  while k = 1 to $M/2$ do
    Crossover operation to population according to $pc = 0.3$;
  end while
  while k = 1 to M do
    Mutation operation to population according to $pm = 0.03$;
  end while
  $k = k + 1$;
end while
Output optimal results.

Algorithm 1: The algorithm for feature selection.

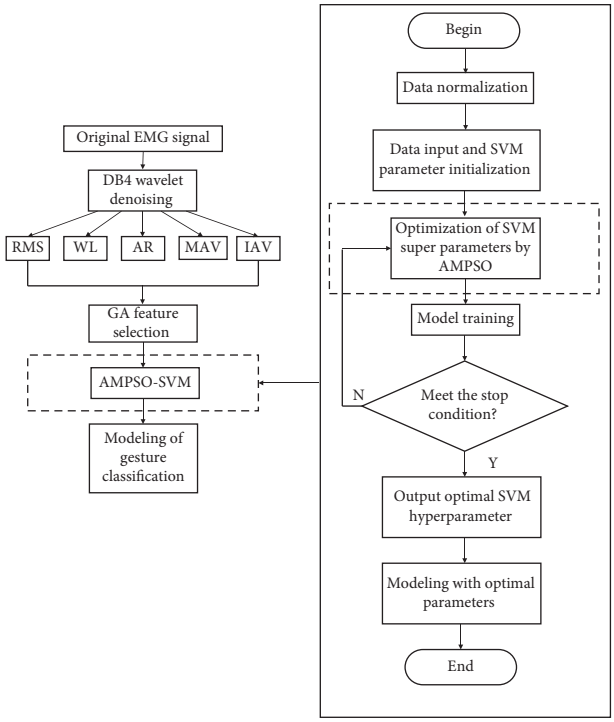

Figure 3: Flowchart of AMPSO-SVM gesture recognition model algorithm.

individual best particle respectively; rand is the random number uniformly distributed in [0, 1]; ω is the inertia weight, maintaining the balance of global and local search capabilities.

Aiming at the premature convergence problem of PSO algorithm, in order to obtain the better SVM parameter selection using PSO algorithm, this paper proposes an adaptive mutation operation after particle position update and defines a new adaptive mutation probability calculation method, so as to obtain an adaptive mutation PSO algorithm.

In the process of iteration, particles continuously fly in the optimal direction. If a particle finds a current optimal position, then other particles quickly approach it, and the speed of all particles drops to zero in a short time. If the optimal particle is a local optimum, then the particle swarm cannot search for the optimal point in the solution space, even though the premature convergence phenomenon occurs, and it is difficult to jump out of the local extremum. In order to deal with the premature convergence phenomenon in the process of PSO, a simple mutation operator is introduced on the basis of the ordinary PSO algorithm. The basic idea is to reinitialize the particles with a certain probability after each update and set the probability as R. In reference [45], a mutation method has been proposed for binary PSO algorithm, $R = 1/N$ is the mutation probability, and N is the data dimension, but, in the process of algorithm iteration, R is a fixed value. Hence, this method cannot adapt to the characteristics of PSO algorithm properly, while PSO is a kind of heuristic algorithm, which needs strong global searchability in the early stage and local searchability in the later stage. Based on the above characteristics, the mutation probability of PSO in the early stage is larger than that in the later stage.

In this paper, we define a novel mutation probability formula as follows:

$$R = 1 - \frac{i}{(N + i)}, \tag{9}$$

where N is the dimension of the data and i is the algebra of the current algorithm iteration. When a new particle is generated, each particle produces a certain mutation probability. According to the analysis, the range of defined mutation probability R gradually decreases from 1 to 0; that is, almost all mutation occurs in the early stage, and few

```
Initialization;
while rand < R do
k = ceil(2 * rand);
end while
  while k == 1 do
    pop(j,k) = (20 − 1) * rand + 1;
end while
  while k == 2 do
    pop(j,k) = (σmax − σmin) * rand + σmin;
  end while
```

Algorithm 2: The algorithm for mutation operation rules.

Initialize:
Set the position parameter v_{id}^k according to formula (7);
Set the speed parameter x_{id}^k according to formula (8);
while $k = 1$ to maximum iterations do
  Calculate the initial *p*best and *g*best, according to the classification accuracy of SVM cross validation;
  Calculate the mutation probability of the current generation of particles according to (9);
  Update the position x_{id}^k and velocity v_{id}^k of each particle in the population according to (7)-(8);
  Perform particle mutation according to the rules;
  Update the individual optimal position *pbest* and the population optimal position *gbest* according to the fitness of particles;
  $k = k + 1$
end while
Output optimal structure C and σ.

Algorithm 3: The algorithm for searching parameters.

mutations occur in the late stage, which can better adapt to the characteristics of PSO algorithm.

The adaptive mutation rules are defined in Algorithm 2:

The implementation steps of the proposed AMPSO-SVM algorithm are in Algorithm 3:

Taking the accuracy of the training set in the sense of CV as the fitness function value in the AMPSO, the overall algorithm process of optimizing SVM parameters by AMPSO is shown in Figure 4.

In this paper, adaptive PSO is used to determine the parameters C and σ that are more suitable for SVM, and the proposed AMPSO-SVM will be used to classify four EMG gestures in Section 4.

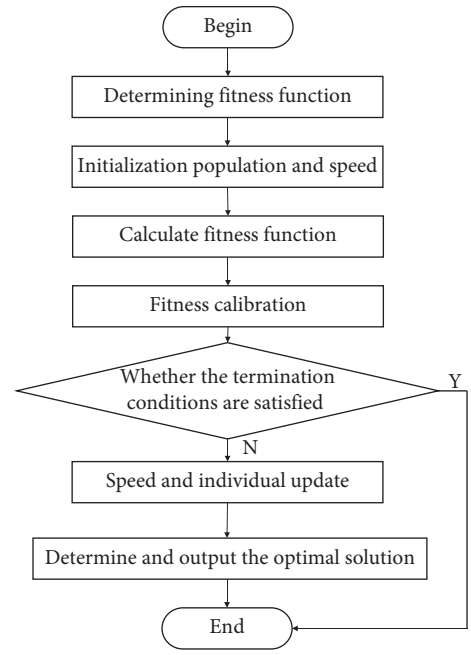

Figure 4: Flowchart of SVM parameters optimized by particle swarm optimization.

4. Experiment and Analysis

4.1. Data Sources. Data utilized in this study were acquired from UCI dataset [46], which adopts a noninvasive method; the dataset is measured by the MYO bracelet worn on the user's forearm. The subjects measured the surface EMG signals of upper limbs by MYO bracelet, viewed the EMG signals by PC software, and then processed the original data by feature extraction, feature selection, and pattern classification.

Now, most of the published datasets use American Delsys electrode and German Otto bock electrode, such as Ninapro [47]. It can be worn above the elbow joint of different people's arms. MYO bracelet has the advantages of stronger mobility, nonrestriction of space and site. The dataset used in this study was collected from 36 healthy volunteers, aged 18 to 41. The bracelet involving eight

sensors is set equidistant around the forearm; moreover, it can simultaneously obtain muscle image signals. Each gesture is executed for 3 seconds, and the pause time between two gestures is 3 seconds.

MYO has eight channels with high dimensions. The sampling frequency of MYO is 200 Hz, and the number of data samples is small. Therefore, MYO has the characteristics of small samples and high dimension. In view of the characteristics of the dataset collected by MYO, it is necessary to study this kind of data.

The experiment evaluates the EMG of these four gestures from two perspectives. The first method is to take all four gesture categories into account to calculate the effectiveness of category prediction. The other method is to consider each category separately and calculate the effectiveness of each category separately. The proposed AMPSO-SVM algorithm is validated and compared with four popular methods including adaptive PSO, ordinary PSO, grid search for SVM parameters (GS-SVM), and BP algorithm.

4.2. Multiclassification. In this section, we randomly select one person from the dataset (http://archive.ics.uci.edu/ml/datasets/EMG+data+for+gestures) to do a classifier verification experiment. Four kinds of gestures were selected from the dataset, such as twist flexion, twist extension, radial deviation, and ulnar deviation. The error classification charts of BP [48], GS-SVM [49], PSO-SVM [50], and AMPSO-SVM are drawn respectively to intuitively understand the four algorithms' classification performance. By observing the sEMG data of 8 channels from the selected person, it seems that the data range of the selected person's ulnar deviation is quite different from the other three actions.

4.2.1. Test Set Classification Result. The classification accuracy of the four recognition methods for the selected person is shown in Figure 5. The results of BP algorithm, GS-SVM algorithm, PSO-SVM algorithm, and AMPSO-SVM algorithm are shown in Figures 5(a)–5(d), respectively.

Figure 5(a) illustrates that BP algorithm is capable of classifying the ulnar deviation and radial deviation; however, the twist flex and twist extension are not identified successfully. As can be seen from Figure 5(a), the recognition rate of BP algorithm is 0.9019. Moreover, the BP algorithm is too complex for inexperienced users due to a large number of layers and parameters.

Then the twist extension can be classified using GS-SVM as shown in Figure 5(b). However, the twist flex has still not been identified in this case. Although the accuracy is improved in this case, the process is expensive for computation. The recognition rate is 0.9093.

In Figure 5(c), it can be seen that the PSO-SVM algorithm is slightly higher than GS-SVM, and the recognition rate is 0.9463. PSO and GA are commonly used as heuristic algorithms. Compared with GA algorithm, PSO has no operation of selection, crossover, and mutation, so its convergence speed is relatively fast. In this paper, PSO algorithm is used to optimize the parameters of SVM. The idea of mutation in GA is also introduced into PSO, which can integrate the advantages of both.

Figure 5(d) illustrates that the classification performance of the proposed AMPSO-SVM has greatly improved compared with the other three recognition methods. The recognition rate of AMPSO-SVM is 0.975. As can be seen from Figure 5, all features have been accurately identified and classified using the proposed AMPSO-SVM algorithm. Moreover, the test set sample labels are predicted as well.

The performance comparison of the four algorithms can be indicated by the recognition rate. The recognition rate of AMPSO-SVM is 0.975, which is the highest from the 0.9019 of BP algorithm, 0.9093 of GS-SVM algorithm, and 0.9463 of PSO-SVM algorithm.

The parameters of the proposed AMPSO-SVM algorithm are set as follows: the maximum number of iterations is 100, the population size is 25 generations, the learning factors $c_1 = 1.6, c_2 = 1.9$, and the mutation probability is $R = 1 - i/N + i$. The curve of the best fitness value with the iteration times in AMPSO-SVM algorithm is shown in Figure 6.

Figure 6 indicates that the adaptive mutation PSO is optimized iteratively and converges in the 13^{th} generation, the SVM parameters can be found as $C = 4.4792$, $\sigma = 0.17226$; moreover, the classification accuracy of four postures reaches 97.5%. Through the comparison of the above results, it can be clearly seen that the parameters found by the adaptive mutation PSO can obtain higher classification accuracy.

4.2.2. Evaluation Indexes. In this section, we will evaluate the effectiveness of the four algorithms in multiclassification tasks based on three evaluation indicators, including accuracy, Kappa coefficient, andMacroF1. Classification accuracy is the most commonly used standard indicator to evaluate the quality of the model. The calculation formula is as follows:

$$\text{accuracy} = \frac{m}{n}, \tag{10}$$

where m is the correct number of samples in the test set and $n$is the total number of samples in the test set.

Kappa coefficient is used to evaluate the reduction of the classification error rate compared with complete random classification. The calculation formula is defined as follows:

$$\text{Kappa} = \frac{\text{accuracy} - p_e}{1 - p_e}, \tag{11}$$

where c is the data category, $t_1, t_2, \ldots, t_c$ are the real sample numbers of each class, $h_1, h_2, \ldots, h_c$ are the predicted sample number of each class, and the calculation formula of p_e can be defined as follows:

$$p_e = \frac{t_1 \times h_1 + t_2 \times h_2 + \cdots + t_c \times h_c}{n \times n}. \tag{12}$$

Kappa coefficient can be divided into five groups to represent different levels of consistency: 0.0 to 0.20 for very low consistency, 0.21 to 0.40 for fair, 0.41 to 0.60 for

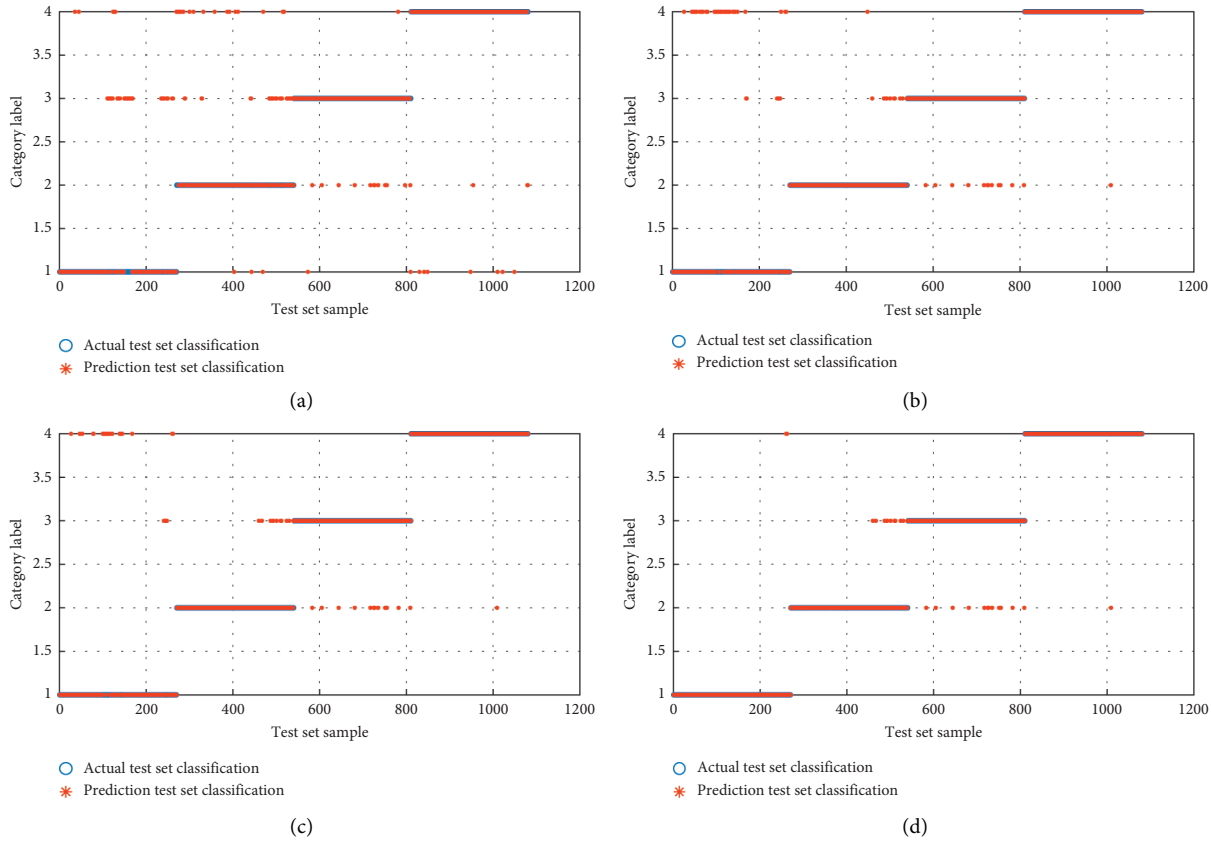

Figure 5: Test set classification graph of the four methods. (a) BP. (b) GS-SVM. (c) PSO-SVM. (d) AMPSO-SVM.

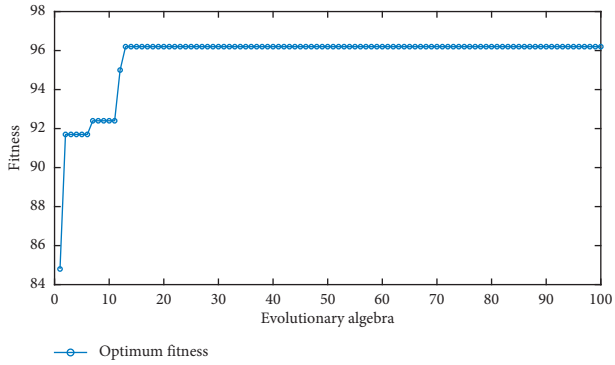

Figure 6: Optimal fitness of adaptive particle mutation PSO.

moderate, 0.61 to 0.80 for substantial, and 0.81 to 1 for almost perfect.

Macro F_1 is the arithmetic mean of each sEMG performance (precision, recall and F_1); G_1, G_2, G_3, and G_4 are used to represent wrist flexion, twist extension, radial deviation, and lar deviation, respectively, and the formula is defined as follows:

$$F_1 = \frac{2\,(\text{precision} \times \text{recall})}{(\text{precision} + \text{recall})}, \tag{13}$$

where F_1 measures the combination of recall and precision of categories G_1, G_2, G_3, and G_4, precision usually is used to measure the precision of categories G_1, G_2, G_3, and G_4, and recall is used to measure recall rate of categories G_1, G_2, G_3, and G_4, respectively.

$$\text{Macro } F_1 = \frac{F_1 + \cdots + F_4}{4}, \tag{14}$$

twhere $F_1 + \cdots + F_4$ is the F_1 from category 1 to category 4.

According to the above three evaluation indicators, it can be seen from Figure 7 that the multiclassification performance of PSO-SVM algorithm is slightly better than GS-SVM algorithm and BP algorithm, while AMPSO-SVM algorithm is obviously the best of all algorithms.

4.3. Classification Performance of Each Action

4.3.1. Different People. In this section, we randomly select five people from the dataset to repeat the experiments five times. Only GS-SVM, PSO-SVM, and AMPSO-SVM are considered in this section to test the classification performance since they are capable of classifying at least three kinds of sEMG. Figure 8 shows the recognition rate of the four actions of these five people. We can see that the recognition rates of the three classifiers for different people are quite different. The results indicate that even though the collected data are significantly affected by different people, the recognition rate of all selected postures using AMPSO-SVM algorithm is still the highest. Moreover, the recognition rates of twist extension and radial deviation using AMPSO-

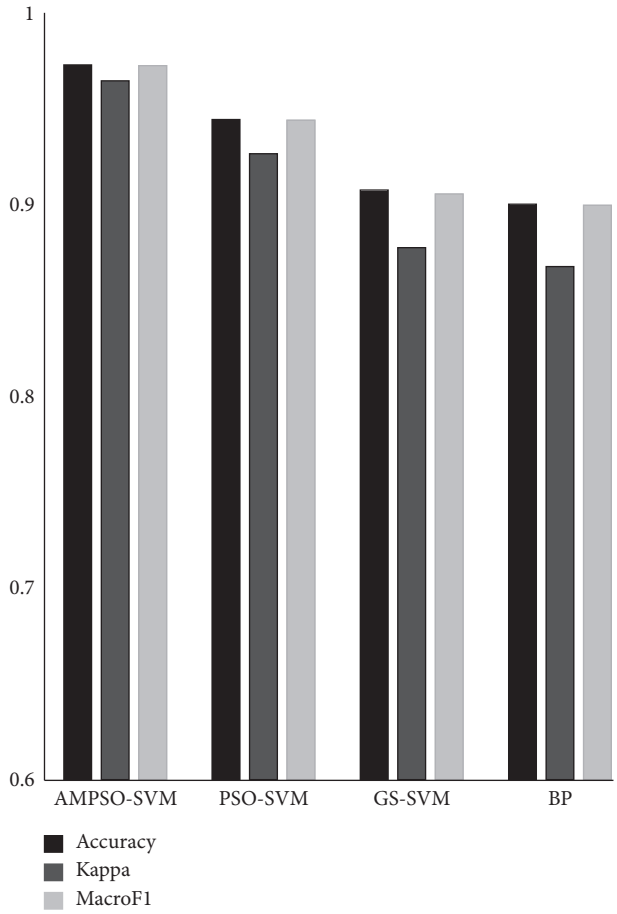

Figure 7: Comparison of four evaluation methods.

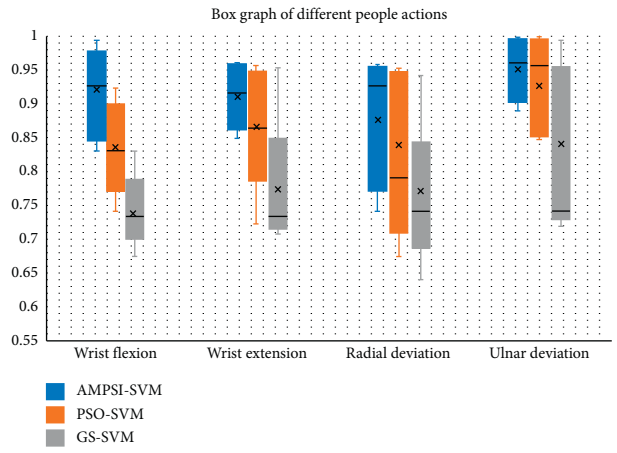

Figure 8: Box graphs of different people.

SVM algorithm are slightly higher than those using PSO-SVM algorithm. Furthermore, the accuracy of the AMPSO-SVM algorithm and PSO-SVM algorithm is closed on recognizing the ulnar deviation.

4.3.2. Average Recognition Rate. The recognition rates of different postures are different due to the different posture performances of subjects. Thus, we calculate the average recognition rate of the five randomly selected people to see the difference among the three classifiers. Figure 9 shows the average recognition rate of the four actions.

The average recognition rate of wrist flexion using AMPSO-SVM algorithm shown in Figure 9(a) is the highest of the three algorithms. The result of AMPSO-SVM is 0.08 higher than that of PSO-SVM. The result in Figure 9(b) is

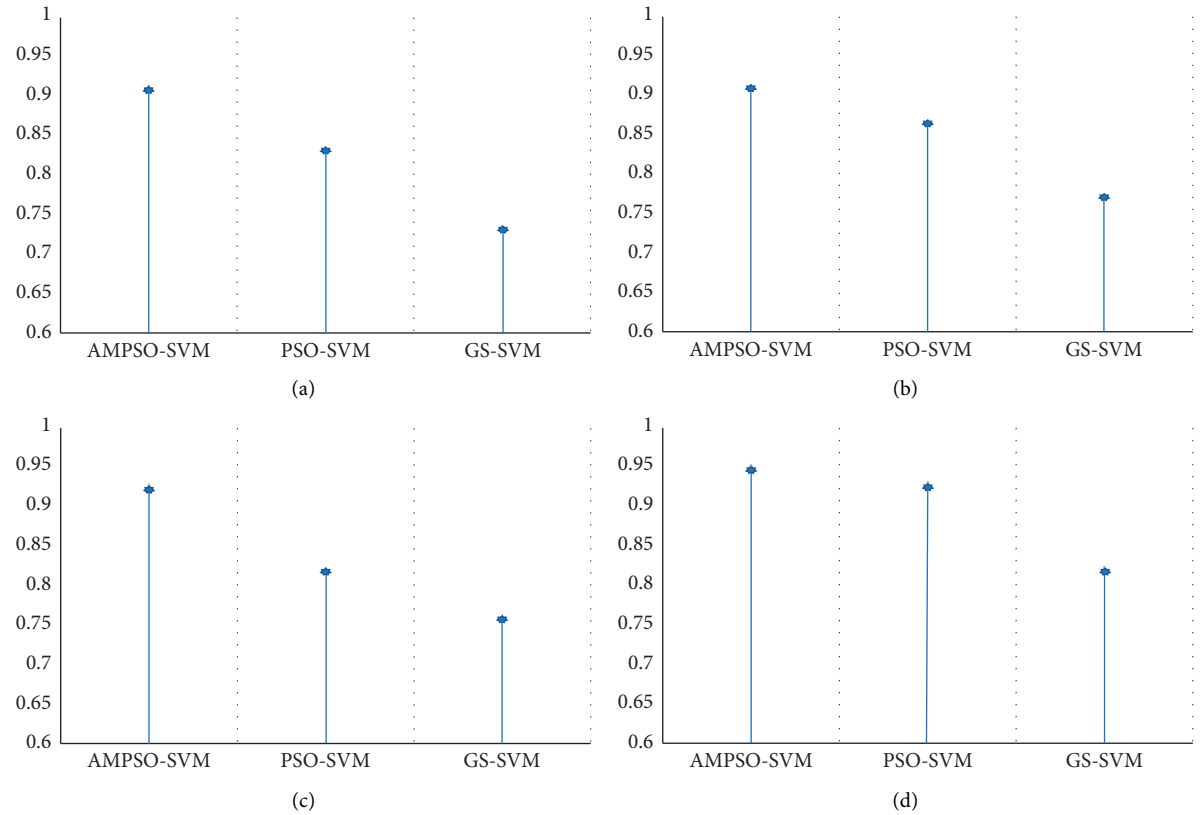

Figure 9: Average recognition rate of four actions. (a) Wrist flexion. (b) Wrist extension. (c) Radial deviation. (d) Ulnar deviation.

similar to the result of wrist extension. The average recognition rate of radial deviation using AMPSO-SVM algorithm is much higher than the value using PSO-SVM algorithm. Moreover, the difference of results between AMPSO-SVM and the other two algorithms used for radial deviation recognition is relatively large as shown in Figure 9(c). Figure 9(d) shows the average recognition rate of ulnar deviation. The result using AMPSO-SVM algorithm is similar to the value using PSO-SVM algorithm, which is higher than the result using GS-SVM. Figure 9 illustrates that the AMPSO-SVM algorithm has the advantage of recognizing the wrist flexion, wrist extension, and radial deviation. However, the capability of PSO-SVM algorithm is similar to the AMPSO-SVM algorithm for recognizing the ulnar deviation.

5. Conclusion

In this paper, a new AMPSO-SVM algorithm is proposed and successfully applied to low sampling rate sEMG gesture recognition. In order to improve the adaptability of gesture recognition technique, a new mutation probability calculation method is defined in particle mutation, which can effectively solve the premature problem of PSO. In the aspect of feature extraction, five features with a high correlation to muscle contraction have been selected. This combination of calculations is simple and fast and can effectively obtain the sEMG signal information. The genetic algorithm is used to solve the problem of high dimension and redundancy of multichannel sEMG signals, which effectively reduces the complexity of subsequent classification. The comparisons of results show that the algorithm is capable of recognizing the sEMG signals with sampling rate accurately. It provides an effective method for gesture recognition of low sampling rate sEMG signal.

Data Availability

The data used in this study can be found at http://archive.ics.uci.edu/ml/datasets/EMG+data+for+gestures.

Conflicts of Interest

The authors declare that there are no conflicts of interest regarding the publication of this paper.

Acknowledgments

The authors would gratefully acknowledge the support by the National Natural Science Foundation of China (NSFC) as the research program (Grant no. 61703270).

References

[1] J. Ben-Arie, Z. Zhiqian Wang, and S. Rajaram, "Human activity recognition using multidimensional indexing," *IEEE Transactions on Pattern Analysis and Machine Intelligence*, vol. 24, no. 8, pp. 1091–1104, 2002.

[2] F. Riillo, L. R. Quitadamo, F. Cavrini et al., "Optimization of EMG-based hand gesture recognition: supervised vs. unsupervised data preprocessing on healthy subjects and transradial amputees," *Biomedical Signal Processing and Control*, vol. 14, no. 1, pp. 117–125, 2014.

[3] D. A. Zlotolow and S. H. Kozin, "Advances in upper extremity prosthetics," *Hand Clinics*, vol. 28, no. 4, pp. 587–593, 2012.

[4] L. Zhang, W. Qi, Y. Hu, and Y. Chen, "Disturbance-observer-based fuzzy control for a robot manipulator using an EMG-driven neuromusculoskeletal model," *Complexity*, vol. 2020, Article ID 8814460, 10 pages, 2020.

[5] X. Kan, D. Yang, L. Cao et al., "A novel PSO-based optimized lightweight convolution neural network for movements recognizing from multichannel surface electromyogram," *Complexity*, vol. 2020, no. 4, 15 pages, Article ID 6642463, 2020.

[6] A. Phinyomark, P. Phukpattaranont, and C. Limsakul, "Feature reduction and selection for EMG signal classification," *Expert Systems with Applications*, vol. 39, no. 8, pp. 7420–7431, 2012.

[7] M. Nebojša, M. Dimitrije, K. Gunter et al., "Vector autoregressive hierarchical hidden Markov models for extracting finger movements using multichannel surface EMG signals," *Complexity*, vol. 2018, no. 1, 12 pages, Article ID 9728264, 2018.

[8] T. Matsubara and J. Morimoto, "Bilinear modeling of EMG signals to extract user-independent features for multiuser myoelectric interface," *IEEE Transactions on Biomedical Engineering*, vol. 60, no. 8, pp. 2205–2213, 2013.

[9] J. Liu and P. Zhou, "A novel myoelectric pattern recognition strategy for hand function restoration after incomplete cervical spinal cord injury," *IEEE Transactions on Neural Systems and Rehabilitation Engineering*, vol. 21, no. 1, pp. 96–103, 2013.

[10] B. Hudgins, P. Parker, and R. N. Scott, "A new strategy for multifunction myoelectric control," *IEEE Transactions on Biomedical Engineering*, vol. 40, no. 1, pp. 82–94, 1993.

[11] D. Graupe and W. K. Cline, "Functional separation of EMG Signals via ARMA identification methods for prosthesis control purposes," *IEEE Transactions on Systems, Man, and Cybernetics*, vol. SMC-5, no. 2, pp. 252–259, 1975.

[12] P. C. Doerschuk, D. E. Gustafon, and A. S. Willsky, "Upper extremity limb function discrimination using EMG signal analysis," *IEEE Transactions on Biomedical Engineering*, vol. 30, no. 1, pp. 18–29, 2007.

[13] R. Chowdhury, M. Reaz, M. Ali, A. Bakar, K. Chellappan, and T. Chang, "Surface electromyography signal processing and classification techniques," *Sensors*, vol. 13, no. 9, pp. 12431–12466, 2013.

[14] Y. Deng, F. Gao, and H. Chen, "Angle estimation for knee joint movement based on PCA-RELM algorithm," *Symmetry*, vol. 12, no. 1, p. 130, 2020.

[15] F. Jahanmiri-Nezhad, P. E. Barkhaus, W. Z. Rymer, and P. Zhou, "Spike sorting paradigm for classification of multichannel recorded fasciculation potentials," *Computers in Biology and Medicine*, vol. 55, pp. 26–35, 2014.

[16] Y. Qian, J. Liang, and W. Pedrycz, "Positive approximation: an accelerator for attribute reduction in rough set theory," *Artificial Intelligence*, vol. 174, no. 9, pp. 597–618, 2010.

[17] M. Simão, N. Mendes, O. Gibaru, and P. Neto, "A review on electromyography decoding and pattern recognition for Human-Machine interaction," *IEEE Access*, vol. 7, pp. 39564–39582, 2019.

[18] Y. Wu, S. Liang, L. Zhang, Z. Chai, C. Cao, and S. Wang, "Gesture recognition method based on a single-channel sEMG envelope signal," *EURASIP Journal on Wireless Communications and Networking*, vol. 35, no. 2018, 2018.

[19] Y. M. Aung and A. Al-Jumaily, "sEMG based ANN for shoulder angle prediction," *Procedia Engineering*, vol. 41, pp. 1009–1015, 2012.

[20] L. Bruzzone and D. F. Prieto, "A technique for the selection of kernel-function parameters in RBF neural networks for classification of remote-sensing images," *IEEE Transactions on Geoscience and Remote Sensing*, vol. 37, no. 2, pp. 1179–1184, 2002.

[21] Y. Rong, D. Hao, X. Han, Y. Zhang, J. Zhang, and Y. Zeng, "Classification of surface EMGs using wavelet packet energy analysis and a genetic algorithm-based support vector machine," *Neurophysiology*, vol. 45, no. 1, pp. 39–48, 2013.

[22] R. M. Singh, V. Ahlawat, S. Chatterji, and A. Kumar, "Comparative analysis of SVM and ANN classifier based on surface EMG signals for elbow movement classification," *Journal of Interdisciplinary Mathematics*, vol. 23, no. 1, pp. 153–161, 2020.

[23] S. Ranaldi, C. De Marchis, and S. Conforto, "An automatic, adaptive, information-based algorithm for the extraction of the sEMG envelope," *Journal of Electromyography and Kinesiology*, vol. 42, pp. 1–9, 2018.

[24] D. Jiang, G. Li, Y. Sun, J. Kong, and B. Tao, "Gesture recognition based on skeletonization algorithm and CNN with ASL database," *Multimedia Tools and Applications*, vol. 78, no. 21, pp. 29953–29970, 2019.

[25] A. Phinyomark, R. N. Khushaba, and E. Scheme, "Feature extraction and selection for myoelectric control based on wearable EMG sensors," *Sensors*, vol. 18, no. 5, p. 1615, 2018.

[26] H. Kawasaki, M. Kayukawa, H. Sakaeda, and T. Mouri, "Learning system for myoelectric prosthetic hand control by forearm amputees," in *Proceedings of the 23rd IEEE International Symposium on Robot and Human Interactive Communication*, pp. 899–904, Edinburgh, UK, August 2014.

[27] R. Merletti, G. L. Cerone, and T. Tutorial, "Tutorial. Surface EMG detection, conditioning and pre-processing: best practices," *Journal of Electromyography and Kinesiology*, vol. 54, Article ID 102440, 2020.

[28] G. Y. Yang, S. X. Wang, and Y. Chen, "SEMG analysis basing on AR model and Bayes taxonomy," *Applied Mechanics and Materials*, vol. 44–47, pp. 3355–3359, 2010.

[29] A. Shakeel, T. Tanaka, and K. Kitajo, "Time-series prediction of the oscillatory phase of EEG signals using the least mean square algorithm-based AR model," *Applied Sciences*, vol. 10, no. 10, Article ID 3616, 2020.

[30] D. C. Tkach, A. J. Young, L. H. Smith, E. J. Rouse, and L. J. Hargrove, "Real-time and offline performance of pattern recognition myoelectric control using a generic electrode grid with targeted muscle RP," *IEEE Transactions on Neural Systems and Rehabilitation Engineering*, vol. 22, no. 4, pp. 727–734, 2014.

[31] A. H. Al-Timemy, G. Bugmann, J. Escudero, and N. Outram, "Classification of finger movements for the dexterous hand prosthesis control with surface electromyography," *IEEE Journal of Biomedical and Health Informatics*, vol. 17, no. 3, pp. 608–618, 2013.

[32] G. R. Naik and H. T. Nguyen, "Nonnegative matrix factorization for the identification of EMG finger movements: evaluation using matrix analysis," *IEEE Journal of Biomedical and Health Informatics*, vol. 19, no. 2, pp. 478–485, 2015.

[33] Y. Li, W. Zhang, Q. Zhang, and N. Zheng, "Transfer learning-based muscle activity decoding scheme by low-frequency sEMG for wearable low-cost application," *IEEE Access*, vol. 9, pp. 22804–22815, 2021.

[34] D. Xiong, D. Zhang, X. Zhao, and Y. Zhao, "Deep learning for EMG-based human-machine interaction: a review," *IEEE/CAA Journal of Automatica Sinica*, vol. 8, no. 3, pp. 512–533, 2021.

[35] S. Guo, M. Pang, B. Gao, H. Hirata, and H. Ishihara, "Comparison of sEMG-Based feature extraction and motion classification Methods for upper-limb movement," *Sensors*, vol. 15, no. 4, pp. 9022–9038, 2015.

[36] A. Hekmatmanesh, H. Wu, and F. Jamaloo, "A combination of CSP-based method with soft margin SVM classifier and generalized RBF kernel for imagery-based brain computer interface applications," *Multimedia Tools and Applications*, vol. 79, no. 25, pp. 17521–17549, 2020.

[37] H. A. Jaber, T. Rashid, and L. Fortuna, "Online myoelectric pattern recognition based on hybrid spatial features," *Biomedical Signal Processing and Control*, vol. 66, no. 5, pp. 1–11, 2021.

[38] Y. Song, D. Wu, W. Deng et al., "MPPCEDE: multi-population parallel co-evolutionary differential evolution for parameter optimization," *Energy Conversion and Management*, vol. 228, no. 2, Article ID 113661, 2021.

[39] D. Wu, H. Liu, J. Xu et al., "An improved quantum-inspired differential evolution algorithm for deep belief network," *IEEE Transactions on Instrumentation and Measurement*, vol. 69, no. 10, pp. 7319–7326, 2020.

[40] L. Shen, H. Chen, Z. Yu et al., "Evolving support vector machines using fruit fly optimization for medical data classification," *Knowledge-Based Systems*, vol. 96, pp. 61–75, 2016.

[41] D. Zeng, S. Wang, Y. Shen, and C. Shi, "A GA-based feature selection and parameter optimization for support tucker machine," *Procedia Computer Science*, vol. 111, pp. 17–23, 2017.

[42] D. Wu, K. Warwick, Z. Ma et al., "Prediction of Parkinson's disease tremor onset using a radial basis function neural network based on particle swarm optimization," *International Journal of Neural Systems*, vol. 20, no. 2, pp. 109–116, 2010.

[43] B. Iason, N. E. Krausz, A. M. Simon et al., "Decoding the grasping intention from electromyography during reaching motions," *Journal of NeuroEngineering and Rehabilitation*, vol. 15, no. 1, pp. 1–13, 2018.

[44] J. Kennedy and R. C. Eberhart, "Particle swarm optimization," in *Proceedings of the IEEE International Joint Conference on Neural Networks*, vol. 4, pp. 1942–1948, Perth, Australia, November 1995.

[45] Y. Zhang, S. Wang, P. Phillips, and G. Ji, "Binary PSO with mutation operator for feature selection using decision tree applied to spam detection," *Knowledge-Based Systems*, vol. 64, pp. 22–31, 2014.

[46] L. Sergey, K. Nadia, and K. Innokentiy, "Latent factors limiting the performance of sEMG-interfaces," *Sensors*, vol. 18, no. 4, Article ID 1122, 2018.

[47] M. Atzori and H. Müller, "The Ninapro database: a resource for sEMG naturally controlled robotic hand prosthetics," *IEEE Engineering in Medicine & Biology Society*, vol. 2015, Article ID 7320041, 7154 pages, 2015.

[48] R. Ma, L. Zhang, G. Li, D. Jiang, S. Xu, and D. Chen, "Grasping force prediction based on sEMG signals," *Alexandria Engineering Journal*, vol. 59, no. 3, pp. 1135–1147, 2020.

[49] M. A. Oskoei and H. Huosheng Hu, "Support vector machine-based classification scheme for myoelectric control applied to upper limb," *IEEE Transactions on Biomedical Engineering*, vol. 55, no. 8, pp. 1956–1965, 2008.

[50] A. Subasi, "Classification of EMG signals using PSO optimized SVM for diagnosis of neuromuscular disorders," *Computers in Biology and Medicine*, vol. 43, no. 5, pp. 576–586, 2013.